Acta Crystallographica Section F
Structural Biology and Crystallization Communications
ISSN 1744-3091

Structure of the MecI repressor from *Staphylococcus aureus* in complex with the cognate DNA operator of *mec*

Martin K. Safo,[a]* Tzu-Ping Ko,[b] Faik N. Musayev,[a] Qixun Zhao,[c] Andrew H.-J. Wang[b] and Gordon L. Archer[c]

[a]Department of Medicinal Chemistry, School of Pharmacy and Institute for Structural Biology and Drug Discovery, Virginia Commonwealth University, Richmond, Virginia 23298, USA, [b]Institute of Biological Chemistry, Academia Sinica, Taipei 11529, Taiwan, and [c]Department of Medicine and Department of Microbiology/Immunology, Virginia Commonwealth University, Richmond, Virginia 23298, USA

Correspondence e-mail: msafo@vcu.edu

Received 10 February 2006
Accepted 15 March 2006

PDB Reference: MecI–*mec* complex, 2d45, r2d45sf.

The dimeric repressor MecI regulates the *mecA* gene that encodes the penicillin-binding protein PBP-2a in methicillin-resistant *Staphylococcus aureus* (MRSA). MecI is similar to BlaI, the repressor for the *blaZ* gene of β-lactamase. MecI and BlaI can bind to both operator DNA sequences. The crystal structure of MecI in complex with the 32 base-pair cognate DNA of *mec* was determined to 3.8 Å resolution. MecI is a homodimer and each monomer consists of a compact N-terminal winged-helix domain, which binds to DNA, and a loosely packed C-terminal helical domain, which intertwines with its counter-monomer. The crystal contains horizontal layers of virtual DNA double helices extending in three directions, which are separated by perpendicular DNA segments. Each DNA segment is bound to two MecI dimers. Similar to the BlaI–*mec* complex, but unlike the MecI–*bla* complex, the MecI repressors bind to both sides of the *mec* DNA dyad that contains four conserved sequences of TACA/TGTA. The results confirm the up-and-down binding to the *mec* operator, which may account for cooperative effect of the repressor.

1. Introduction

The versatile microorganisms of the staphylococci cause a number of human diseases, from mild inflammation of wounds to diarrhea, pneumonia and toxic shock syndrome, which can be life-threatening. The extensive use of antibiotics in treatment of infections has led to the emergence of *Staphylococcus aureus* strains that are resistant to virtually all known antibiotics, including the most potent, methicillin (Farr, 2004). In general, the β-lactam antibiotics kill bacteria by binding to and inhibiting a class of penicillin-binding proteins (PBPs) that are involved in cell-wall biosynthesis (Goffin & Ghuysen, 2002). Previous studies of methicillin-resistant *S. aureus* (MRSA) showed that the bacteria acquire resistance by incorporating a transportable genetic element of staphylococcal chromosomal cassette SCC*mec*, which contains the *mecA* gene that encodes a novel PBP-2a with reduced affinity for β-lactam antibiotics (Enright, 2003). The crystal structures of a number of PBPs have been determined, including a PBP-2a from an MRSA strain (Lim & Strynadka, 2002).

On the other hand, resistance towards β-lactam antibiotics is conferred in part by β-lactamase, the known crystal structures of which serve as a basis for drug design (Sandanayaka & Prashad, 2002). The production of PBP-2a and β-lactamase are regulated by the repressors MecI and BlaI, which bind to the operators of *mec* and *bla*. MecI and BlaI function as homodimers and are highly homologous. Both contain a winged-helix domain and a helical dimerization domain (Garcia-Castellanos *et al.*, 2003; Safo *et al.*, 2005) and are interchangeable in binding to either of the operator DNA sequences (McKinney *et al.*, 2001). The crystal structures of MecI–*bla* and BlaI–*mec* complexes show that the repressors interact with the TACA/TGTA core sequences primarily *via* the recognition helix α3 (Garcia-Castellanos *et al.*, 2004; Safo *et al.*, 2005). The genes of *mec* and *bla* also encode the membrane-bound sensors MecR1 and BlaR1 that bind to β-lactam antibiotics and cleave the repressors at a specific site in the dimerization domain (Zhang *et al.*, 2001). The truncated

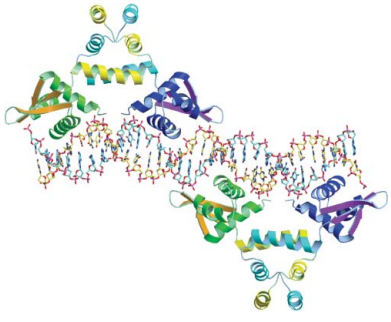

repressors can no longer bind to the DNA and gene expression is promoted. Two crystal structures of the β-lactamase-like BlaR1 sensor domains are known (Kerff *et al.*, 2003; Wilke *et al.*, 2004), but it remains to be determined how the signal is transmitted through the cell membrane and how the protease recognizes the specific cleavage site.

The crystal structure of BlaI–*mec* shows that the repressors are bound to alternate sides of the operator DNA (Safo *et al.*, 2005). It explains the 43–46 bp DNA sequence protected by the repressor from DNase I digestion and suggests a possible mechanism of cooperative binding through the protein–DNA interactions across the DNA dyad. Presumably, MecI binds to *mec* in a similar manner. In this paper, we determine a new trigonal crystal structure of the MecI–*mec* complex that further confirms the up-and-down binding mode.

2. Materials and methods

2.1. Protein purification

The gene *mecI* encoding the repressor protein was amplified by PCR as described previously (McKinney *et al.*, 2001). The PCR products were digested with *Nco*I and *Bam*HI and the DNA fragments were cloned into pET3 (Novagen). This construct was transferred into *Escherichia coli* strain B834 (DE3) (Novagen) competent cells and DNA sequencing was performed to confirm the appropriate orientation of the inserted gene. MecI was then overexpressed in *E. coli* B834 (DE3) in 6 l of M9 defined medium (2 m*M* $MgSO_4$, 0.4% glucose, 0.1 m*M* $CaCl_2$, 1 g l^{-1} thiamine hydrochloride, 40 mg l^{-1} of all amino acids except for methionine, 100 mg l^{-1} ampicillin and 40 mg l^{-1} selenomethionione) at 310 K with 0.5 m*M* IPTG as inducer.

The harvested cells were solubilized in 20 m*M* phosphate buffer pH 6.8 by sonification and the crude lysate was precipitated with 60–90% ammonium sulfate. The precipitate was dissolved in 20 m*M* phosphate buffer pH 6.8 and dialyzed overnight at 277 K against the same phosphate buffer. Following dialysis, the protein extract containing MecI was loaded onto a Mono-S affinity column (Amersham-Pharmacia) pre-equilibrated with 20 m*M* phosphate buffer pH 6.8. The column was washed with the equilibration buffer for 30 min. Protein elution was started with a linear gradient of NaCl in the equilibration buffer and MecI was eluted from the column when the NaCl concentration reached 0.7 m*M*. The purification procedure was carried out at room temperature. The eluted fractions that contained MecI were identified by Western blotting and concentrated using a Centricon YM-3 column (Millipore). About 15 mg purified MecI was obtained with a purity greater than 99% as determined by SDS–PAGE.

2.2. Crystallization and data collection

Several complementary oligonucleotides from the *mec* palindromic operator, including 24, 26, 28 and 32 bp sequences, were used in the initial crystallization trials. The oligonucleotides were purchased from Integrated DNA Technologies (Coralville, Iowa, USA) and were dissolved in STE buffer (10 m*M* Tris pH 8.0, 50 m*M* NaCl, 1 m*M* EDTA) at a concentration of 10 OD_{260} units per 100 µl. The two strands were mixed in equal molar amounts, heated to 367 K and gradually cooled to room temperature to give double-stranded DNA. X-ray-quality crystals were only obtained from the 32 bp DNA (5′-GACTACATTTGTAGTATATTACAAATGTAGTA-3′ and its complement 5′-TACTACATTTGTAATATACTACAAATGTAGTC-3′).

For crystallization, SeMet-incorporated MecI (15 mg ml^{-1} in 20 m*M* K_2HPO_4/KH_2PO_4 pH 6.8, 0.3 *M* NaCl) and 32 bp dsDNA (0.78 m*M* in 10 m*M* Tris pH 8.0, 50 m*M* NaCl, 1 m*M* EDTA) were mixed in approximately a 1:1.5 ratio and incubated for several hours at 277 K. Initial crystallization experiments were carried out by the hanging-drop vapor-diffusion method using the Natrix and Crystal Screen I and II screening protocols from Hampton Research. The volume of the crystallization drop was 4 µl, composed of 2 µl MecI–*mec* complex solution and 2 µl reservoir solution, and was equilibrated against 1 ml reservoir solution. Small irregular crystals were obtained in 2–3 d when PEG was used as precipitating agent. Attempts to improve the quality of these crystals were performed by using different molecular-weight PEGs and varying the pH of the solutions. The best results were obtained using a solution of 80 m*M* Na HEPES pH 7.2, 24% PEG 400 and 150 m*M* $MgCl_2$. However, after two weeks crystal growth stopped. A repeated macroseeding technique was used to improve the crystal dimensions to approximately 0.05 × 0.05 × 0.1 mm. All crystallization experiments were performed at room temperature, whereas data collection took place at 100 K. Prior to storage in liquid nitrogen, crystals were soaked for a few seconds in cryoprotectant solution (0.1 *M* Na HEPES pH 7.2, 0.2 *M* $MgCl_2$ and 35% PEG 400). X-ray data were collected at the National Synchrotron Light Source at 100 K. The intensity data were processed and scaled using the *HKL*2000 package (Otwinowski & Minor, 1997). Statistics are shown in Table 1.

Table 1
Data-collection and refinement statistics of the MecI–*mec* complex crystal.

Values in parentheses are for the outermost resolution shell.

Data collection	
Space group	$P3_212$
Unit-cell parameters (Å)	a = 61.46, b = 61.46, c = 419.78
Resolution (Å)	40–3.8 (3.94–3.80)
No. of observations	90583 (4967)
Unique reflections	9437 (903)
Completeness (%)	99.8 (98.5)
Average $I/\sigma(I)$	33.9 (2.9)
R_{merge} (%)	8.1 (47.0)
Refinement	
No. of reflections†	9168 (797)
R value based on 95% of data	0.264 (0.326)
R_{free} based on 5% of data	0.297 (0.308)
R.m.s.d. bond lengths (Å)	0.017
R.m.s.d. bond angles (°)	1.6
No. of non-H atoms	
Protein atoms	3958
DNA atoms	1166
Water molecules	80
Average B values (Å^2)	
Protein atoms	115.0
DNA atoms	132.1
Water molecules	68.7
Ramachandran plot: residues (excluding prolines and glycines)	
In most favored regions	362 [81.5%]
In allowed regions	78 [17.6%]
In disallowed regions	4 [0.9%]

† All positive reflections were used in the refinement.

2.3. Structure determination and refinement

A model that contained 16 base pairs of DNA and a BlaI dimer derived from PDB code 1xsd was used in a molecular-replacement search employing *AMoRe* (Navaza, 2001; Collaborative Computational Project, Number 4, 1994). Two clear solutions indicated that the trigonal crystal of MecI–*mec* belongs to space group $P3_212$ and contains about 52% solvent volume. Rigid-body refinement with *CNS* (Brünger *et al.*, 1998) yielded an R value of 0.437 at 3.8 Å resolution, which became 0.401 by replacing the BlaI models with MecI from PDB code 1sax. The protein model contains residues 5–121, 3–121,

5–121 and 7–121 for the four chains *A*, *B*, *C* and *D*, respectively. Owing to the low resolution of the data set, the DNA sequence could not be resolved and was represented by TACTACATATGTAGTA as an average (Safo *et al.*, 2005). Seven nucleotides at the open ends of the DNA duplex lacked electron density in the $2F_o - F_c$ maps and were removed. Prior to further refinement, 5% of the data were reserved for calculation of R_{free} as a monitor (Brünger, 1993). Equivalent atoms were treated with strong non-crystallographic symmetry restraints. The final R and R_{free} values of 0.264 and 0.297, respectively, are high, most likely owing to the low-resolution data as well as disorder in the DNA. The final model contains residues *A*5–121, *B*3–121, *C*5–121 and *D*7–121 for protein and *A*201–216, *B*201–216, *C*201–213 and *D*205–216 for DNA. There are 80 water molecules in the final model and a number of these were added to accommodate what we interpret as remnant densities of highly disordered DNA. After refinement, the four MecI monomers have root-mean-squares deviations (r.m.s.d.s) from each other of 0.359–0.422 Å for 991 non-H atoms. The DNA strands deviate by an r.m.s.d. of 0.283–0.403 Å between 204 equivalent atoms. Other refinement statistics are shown in Table 1. All figures were produced using *MolScript* (Kraulis, 1991) and *Raster3D* (Merritt & Murphy, 1994).

3. Results and discussion

The asymmetric unit of the trigonal crystal contains two MecI dimers bound separately to two DNA segments. One of the DNA segments consists of a 16-base-pair duplex; the other contains 12 base pairs and an unpaired nucleotide. The former is parallel to the *ab* diagonal of the unit cell (horizontal) and the latter is parallel to the *c* axis (vertical). By crystallographic symmetry operations, both segments can be extended to generate the 32 bp DNA of the *mec* operator used in crystallization, as shown in Figs. 1(*a*) and 1(*b*), whereas the termini of the vertical segment are disordered. Each 32 bp DNA includes four consensus TACA/TGTA motifs for repressor binding and indeed there are two MecI dimers bound on the opposite sides. Furthermore, by lattice translation, the horizontal DNA segment forms a long virtual double-stranded DNA as shown in Fig. 1(*c*).

In the current structure, adjacent up-and-down dimers cover a 42 bp length on the DNA, consistent with DNase I footprint studies that indicate that the repressors bind to the *mec* operator protecting a single 43–46 bp sequence (Sharma *et al.*, 1998). As noted previously for the BlaI–*mec* complex structure (Safo *et al.*, 2005), the cooperative binding of MecI to the *mec* promoter-operator (Sharma *et al.*, 1998) could arise from the fact that binding of the first MecI dimer may lead

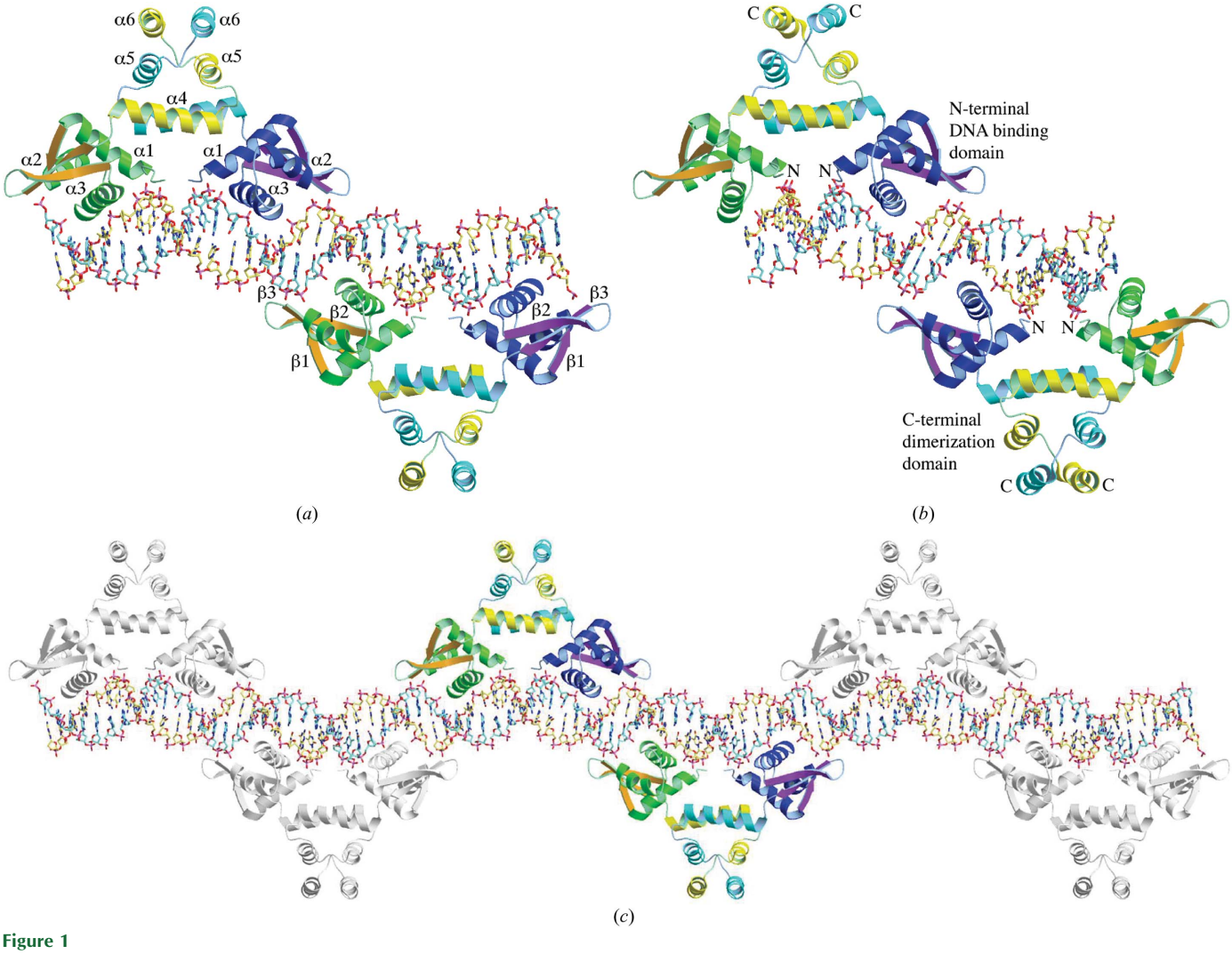

Figure 1
Overall structures of the MecI–*mec* complex. (*a*) The horizontal 32 bp DNA fragment of the *mec* operator with two dimeric MecI repressors bound. The DNA molecule is shown as sticks and the protein as ribbons, with α-helices and β-strands labeled in the 'up' and 'down' dimers, respectively. (*b*) The vertical 24 bp DNA fragment with unpaired 3′-ends, also bound to two repressors. (*c*) The virtual double helix formed by the horizontal DNA fragments *via* lattice translations of the trigonal crystal.

to perturbation of the DNA double helix that makes the opposite side of the DNA more accessible to a second dimer. Specifically, interactions between the protein and DNA across the dyad DNA axis may produce slight deviations from the canonical B-form DNA in this region and thus account for the cooperative binding. In fact, like the BlaI–*mec* complex structure (Safo *et al.*, 2005), we also observe a slight bend in the DNA conformation in the MecI–*mec* complex structure.

Each monomer of the dimeric MecI contains an N-terminal DNA-binding domain and a C-terminal dimerization domain. The three α-helices in the C-terminal domain are intertwined to constitute the dimer interface, with similar interdimer interactions. The N-terminal domain comprises of three α-helices and three antiparallel β-strands, typical of the winged-helix DNA-binding proteins (van Melckebeke *et al.*, 2003). The protein–DNA interactions are similar to those observed previously for the DNA-bound MecI and BlaI structures (Garcia-Castellanos *et al.*, 2003, 2004; Safo *et al.*, 2005), including three sequence-specific hydrogen bonds from Thr47 to Ade213 and from Arg51 to both Gua211 and Thy212. Other contacts between the protein and mostly the DNA backbone involve Ser9, Ser10 (Met in BlaI), Ala11, Ser41, Thr44, Thr47, Leu48, Lys43, Arg60, Arg44, Asn28, Lys65 and Phe67 (Tyr in BlaI).

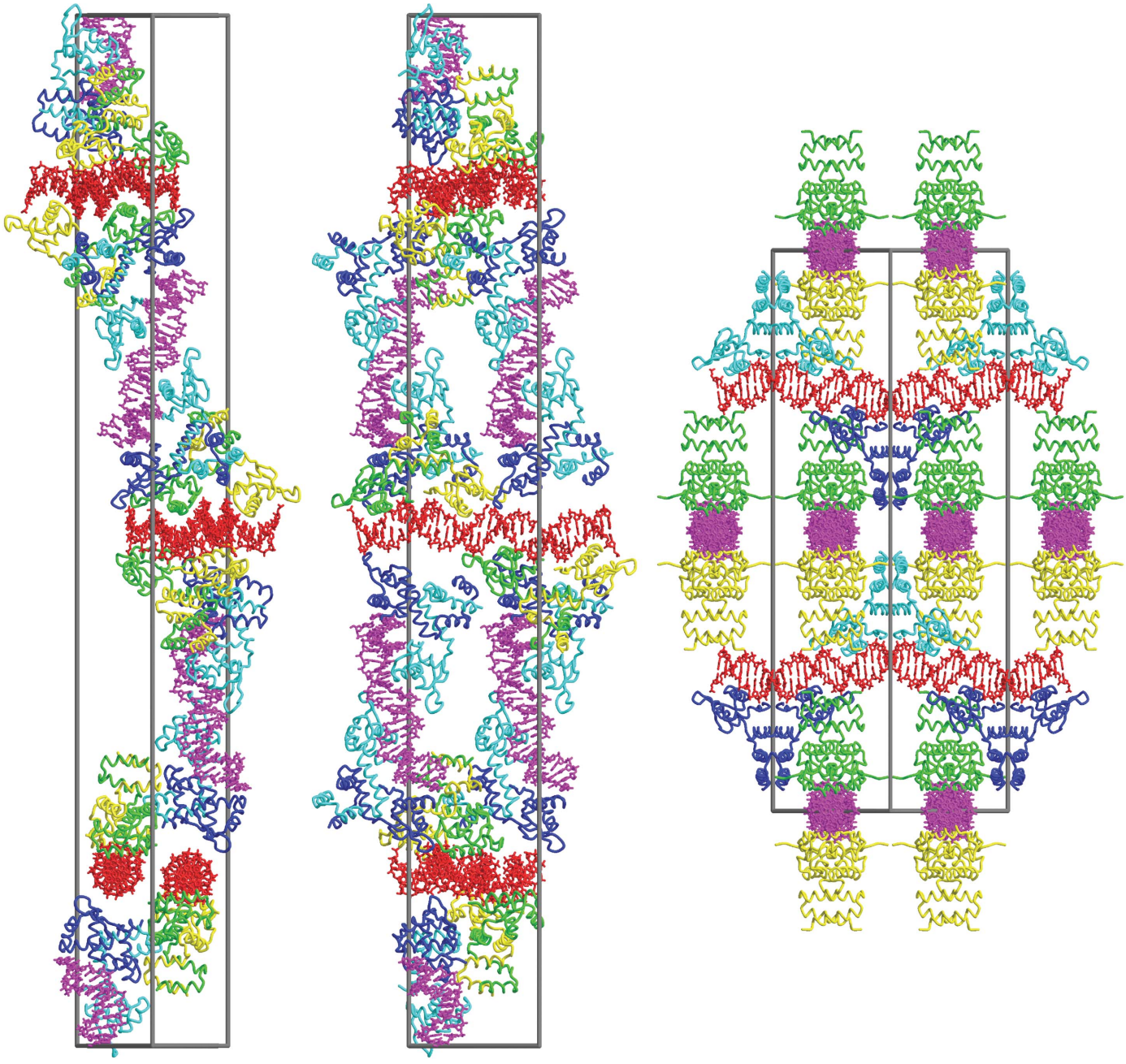

Figure 2
Packing of the MecI–*mec* and BlaI–*mec* crystals. (*a*) Unit-cell content of the trigonal MecI–*mec* crystal viewed along the [110] direction. (*b*) Another view by 90° rotation about the *c* axis. Some molecules are removed and additional symmetry-related molecules are included to show the virtual double strands formed by the horizontal DNA segments. (*c*) BlaI–*mec* complexes in the tetragonal crystal (PDB code 1xsd).

We also determined two crystal structures of the native MecI and a selenomethionine derivative (PDB codes 1sd6 and 1sd7), both with slightly different unit-cell parameters from those of PDB code 1okr. Unlike BlaI, which shows a closed-to-open conformational change upon DNA binding, MecI seems to maintain an open conformation, with an overall r.m.s.d. of 1.36–1.61 Å between 936 equivalent backbone atoms in the bound and unbound dimers.

In the trigonal crystal structure of the MecI–*mec* complex studied here, horizontal layers of virtual DNA double helices, with the MecI dimers bound alternately to both sides, are disposed in three orientations differing by 60°. Between these horizontal layers, the vertical DNA segments each with two bound MecI dimers fill the large interlayer space, as shown in Figs. 2(*a*) and 2(*b*). The open ends of the vertical DNA segments lack the stacking interactions observed for those between the horizontal segments and are consequently disordered. In the previous tetragonal crystal structure of the BlaI–*mec* complex (PDB code 1xsd), similar horizontal DNA strands propagate in two perpendicular directions, as shown in Fig. 2(*c*). Direct protein–protein contacts also resulted in a smaller *c*-axis dimension of 243.47 Å. Despite the larger solvent content of 72%, the orthogonal architecture of the BlaI–*mec* crystal yielded higher resolution data.

4. Conclusion

Owing to the disorder and heterogeneity of DNA and the long *c* axis of the unit cell, crystals of the MecI–*mec* complex only diffracted to a limited resolution of 3.8 Å. Nevertheless, this structure confirms the up-and-down mode of MecI repressor binding to the *mec* operator, which explains the 43–46 bp DNA sequence protected from DNase I digestion. The same repertoire as employed in BlaI for binding to *mec* is observed for MecI. The cooperative binding of MecI to the *mec* promoter-operator is likely to occur *via* the protein–DNA interactions through the DNA dyad.

This work was supported by NIH grant AI035705-11 (GLA). Data for this study were measured at beamline X29 of the National Synchrotron Light Source. Financial support comes principally from the Offices of Biological and Environmental Research and of Basic Energy Sciences of the US Department of Energy and from the National Center for Research Resources of the National Institutes of Health. We also thank Howard Robinson, the beamline scientist at X29, for his help in obtaining the data set.

References

Brünger, A. T. (1993). *Acta Cryst.* D**49**, 24–36.
Brünger, A. T., Adams, P. D., Clore, G. M., DeLano, W. L., Gros, P., Grosse-Kunstleve, R. W., Jiang, J.-S., Kuszewski, J., Nilges, M., Pannu, N. S., Read, R. J., Rice, L. M., Simonson, T. & Warren, G. L. (1998). *Acta Cryst.* D**54**, 905–921.
Collaborative Computational Project, Number 4 (1994). *Acta Cryst.* D**50**, 760–763.
Enright, M. C. (2003). *Curr. Opin. Pharmacol.* **3**, 474–479.
Farr, B. M. (2004). *Curr. Opin. Infect. Dis.* **17**, 317–322.
Garcia-Castellanos, R., Mallorqui-Fernandez, G., Marrero, A., Potempa, J., Coll, M. & Gomis-Ruth, F. X. (2004). *J. Biol. Chem.* **279**, 17888–17896.
Garcia-Castellanos, R., Marrero, A., Mallorqui-Fernandez, G., Potempa, J., Coll, M. & Gomis-Ruth, F. X. (2003). *J. Biol. Chem.* **278**, 39897–39905.
Goffin, C. & Ghuysen, J. M. (2002). *Microbiol. Mol. Biol. Rev.* **66**, 702–738.
Kerff, F., Charlier, P., Colombo, M. L., Sauvage, E., Brans, A., Frere, J. M., Joris, B. & Fonze, E. (2003). *Biochemistry*, **42**, 12835–12843.
Kraulis, P. J. (1991). *J. Appl. Cryst.* **24**, 946–950.
Lim, D. & Strynadka, N. C. (2002). *Nature Struct. Biol.* **9**, 870–876.
McKinney, T. K., Sharma, V. K., Craig, W. A. & Archer, G. L. (2001). *J. Bacteriol.* **183**, 6862–6868.
Melckebeke, H. van, Vreuls, C., Gans, P., Filee, P., Llabres, G., Joris, B. & Simorre, J.-P. (2003). *J. Mol. Biol.* **333**, 711–720.
Merritt, E. A. & Murphy, M. E. P. (1994). *Acta Cryst.* D**50**, 869–873.
Navaza, J. (2001). *Acta Cryst.* D**57**, 1367–1372.
Otwinowski, Z. & Minor, W. (1997). *Methods Enzymol.* **276**, 307–326.
Safo, M. K., Zhao, Q., Ko, T.-P., Musayev, F. N., Robinson, H., Scarsdale, N., Wang, A. H.-J. & Archer, G. L. (2005). *J. Bacteriol.* **187**, 1833–1844.
Sandanayaka, V. P. & Prashad, A. S. (2002). *Curr. Med. Chem.* **9**, 1145–1165.
Sharma, V. K., Hackbarth, C. J., Dickinson, T. M. & Archer, G. L. (1998). *J. Bacteriol.* **180**, 2160–2166.
Wilke, M. S., Hills, T. L., Zhang, H. Z., Chambers, H. F. & Strynadka, N. C. (2004). *J. Biol. Chem.* **279**, 47278–47287.
Zhang, H. Z., Hackbarth, C. J., Chansky, K. M. & Chambers, H. F. (2001). *Science*, **291**, 1962–1965.